Journal of Molecular Liquids 371 (2023) 121097

Contents lists available at ScienceDirect

Journal of Molecular Liquids

journal homepage: www.elsevier.com/locate/molliq

Tribological enhancement of potential electric vehicle lubricants using coated TiO_2 nanoparticles as additives

José M. Liñeira del Río [a,b,*], Fátima Mariño [a], Enriqueta R. López [a], David E.P. Gonçalves [b], Jorge H.O. Seabra [c], Josefa Fernández [a]

[a] Laboratory of Thermophysical and Tribological Properties, Nafomat Group, Department of Applied Physics, Faculty of Physics and Institute of Materials (iMATUS), Universidade de Santiago de Compostela, 15782 Santiago de Compostela, Spain
[b] Unidade de tribologia, vibraçoes e manutençao industrial, INEGI, Universidade do Porto, Porto, Portugal
[c] FEUP, Faculdade de Engenharia da Universidade do Porto, Rua Dr. Roberto Frias s/n, 4200-465 Porto, Portugal

ARTICLE INFO

Article history:
Received 22 September 2022
Revised 7 December 2022
Accepted 15 December 2022
Available online 17 December 2022

Keywords:
Low-viscosity lubricants
Transmission fluids
Nanoparticles coating
Friction
Wear

ABSTRACT

This work presents the antifriction and antiwear properties of TiO_2 nanoparticles coated with oleic acid, TiO_2-OA, as additives of a low viscosity polyalphaolefin base oil, PAO8. To find the optimal concentration of nanoadditives that minimize friction and wear, four PAO8 based nanodispersions were formulated: PAO8 + 0.10 wt% TiO_2-OA, PAO8 + 0.25 wt% TiO_2-OA, PAO8 + 0.35 wt% TiO_2-OA and PAO8 + 0.50 wt% TiO_2-OA. Tribological experiments were performed under pure sliding and rolling-sliding conditions at 120 °C, with the four formulated nanolubricants and with PAO8 base oil. All the nanolubricants showed lower friction coefficients than that obtained with the PAO8 base oil, reaching maximum reductions for the 0.35 wt% TiO_2-OA nanolubricant, for both types of test conditions. The tribological specimens tested under pure sliding conditions with the nanolubricants showed fewer wear than those tested with PAO8, finding the highest wear decreases also with the PAO8 + 0.35 wt% TiO_2-OA nanolubricant, being 26 %, 65 % and 73 %, in wear track width, depth and area, in that order. Through Raman microscopy and roughness study of the worn samples, it can be inferred that tribofilm, mending and polishing mechanisms occur. Moreover, the thermal conductivity of the optimal nanolubricant (0.35 wt%) was measured at 20, 30, 40 and 50 °C.

1. Introduction

Globally, transportation is one of the main contributors to CO_2 emissions, producing 28 % of total emissions [1]. In this regard, it is estimated that the CO_2 global emissions produced by vehicles with internal combustion engines (ICE) are between 4 and 5 times higher than by electric vehicles (EVs) when the electrical energy is provided through renewable sources [2]. Electric vehicles (EVs) have dramatically increased in popularity and are leading to a greener future for the automotive industry [1]. A remarkable example is the fact that United Kingdom's government is set to prohibit new fossil fuel vehicle manufacture by 2030 [2]. It is estimated that this would help decrease car gas emissions, only in that country, to the equivalent of almost 50 million tons of CO_2 [2]. Although EVs have a substantial high efficiency in terms of energy consumption, there is a challenge to improve the efficiency even more. Thus, being very efficient and generating very little gas emissions, the effectiveness and resilience 2 problems of EVs lie in the moving components and, consequently, in their tribology. By decreasing friction in elements like gears and bearings, tribology can increase the EVs range of driving. According to the hardware designs of hybrid electric vehicles (HEVs) and full EVs, the electric motor can be placed in different positions [3,4]. If it is integrated within the transmission housing, the lubricant is in contact with the motor and must satisfy different requirements, such as compatibility with the materials of the motor structure and the housing, magnetic compatibility, prevention of cooper corrosion, and good heat transfer characteristics to cool the electric motor [3,5,6]. In comparison to traditional ICE vehicles, mechanical elements of EVs work at higher loads, speeds, temperatures, and under electromagnetic fields [2,7]. These facts imply that electrical and thermal properties of the transmission fluids should be taking into account apart from traditional fluid properties [7]. These peculiarities require the use of a low-viscosity lubricant to act the high speeds of the electric motor [2]. All this, without losing sight of the fact that an effective electric vehicle transmission oil must provide high antiwear performance, at extremely low viscosities. Today, in

* Corresponding author.
E-mail address: josemanuel.lineira@usc.es (J.M. Liñeira del Río).

https://doi.org/10.1016/j.molliq.2022.121097
0167-7322/

EV and HEV models conventional automatic transmission fluids for ICE vehicles are being used with acceptable performance, but these fluids have not been specifically formulated to verify the HEV/EV requirements [8]. Thus, in order to achieve the requirements for coming EVs lubricants, it is essential to use efficient additives to base oils [9]. In this regard, the study of nanomaterials as additives can lead to the advancement of a recent production of lubricants with low viscosity particularly designed to the needs of the new and future EV electric drivelines. Nanomaterials have good tribological properties, high thermal conductivity and can be ecologically friendly in contrast to other conventional additives [10]. Several nanomaterials used as additives of conventional ICE lubricants have shown success in decreasing the friction and wear [11–13]. Nevertheless, studies on their performance in terms of EVs' tribological conditions are scarce. In this aim, Mustafa et al. [2] reviewed some few articles on low-viscosity nanolubricants, among them those based on low-viscosity polyalphaolefins (PAOs). Kalin et al. [14] examined the antifriction and antiwear performance of PAO using MoS_2 nanotubes like additives, discovering significant improvements in friction and wear. PAOs are usually utilized in numerous industrial areas, as automotive engine oils, vehicle gear oils, dielectric fluids, electronics cooling and automotive automatic transmission fluids. In comparison to mineral oils, PAOs show greater chemical and physical properties as better fluidity at low temperature, lower volatility, higher viscosity index, a lower pour point, improved oxidative/thermal stability, lower toxicity, and are biodegradable for low viscosity grades.

In spite of the several developments that have been reached with nanopowders in the area of lubricants, there is yet an important difficulty with the nanodispersions stability due to sedimentation, because nanopowders have a tendency to agglomerate each other [15]. This fact is even more accentuated in low-viscosity lubricants. Chen et al. [15] reviewed the temporal stability of several nanolubricants. They study various characteristics of nanoparticles like their size or the surface modification agent, concluding that the surface modification is vital to efficiently disperse nanopowders in a lubricant oil.

Given those requirements, it is crucial to develop and study possible lubricants formed by low-viscosity base oils and modified nanoparticles as additives. In this work, the key objective is to analyze the tribological properties of TiO_2 nanoparticles with an oleic acid coating, TiO_2-OA, as additives of a low-viscosity base oil (PAO8). Non-coated TiO_2 nanoparticles have shown good tribological properties as additives of an engine lubricant and a vegetable oil [16,17]. Thus, Birleauno et al. [16] recently examined the addition of TiO_2 nanoparticles and a surfactant to 10W30 engine oil, observing that the nanoparticles can improve the friction reduction and the antiwear properties of the neat lubricant. Moreover, Cortes et al. [17] researched the lubrication behavior of a sunflower oil containing non-coated SiO_2 and TiO_2 nanopowders. They observed that the friction coefficient was reduced thanks to adding SiO_2 and TiO_2 nanoparticles around 80 % and 95 %, respectively comparing to the sunflower oil and that the loss of volume was dropped by around 75 % and 70 %, respectively.

2. Material and methods

2.1. Materials

Polyalphaolefin 8, PAO8, was kindly supplied by REPSOL. This sample possesses a dynamic viscosity and density at 313.15 K of 39.47 mPa·s and 0.8163 g·cm^{-3}, respectively, as well as a 138 viscosity index. Infrared spectroscopy (FTIR) was used to characterized PAO8. Fig. 1 reveals a weak peak at 770 cm^{-1} associated to C—C alkyl chains, a peak at 1510 cm^{-1} owing to the C—H bending, two robust peaks around 2850 and 2920 cm^{-1} which correspond to the C—H stretching [25,35]. It can be noted that there is no presence of signals attributed for C=C bonds.

Regarding the nanoadditives, TiO_2 nanoparticles coated with oleic acid (TiO_2-OA) were synthesized using commercial TiO_2, purity: 99.9 % and diameter of 5 nm, which were provided by US Research Nanomaterials, Inc. The TiO_2 nanopowders have been coated with OA following the subsequent reaction:

$$TiO_2 + OA \xrightarrow[1.\ 60^{\circ}C,\ min \quad 2.\ 95^{\circ}C,\ reflux,\ 2h]{NaOH} TiO_2\text{-}OA$$

200 mg of commercial TiO_2 nanopowder were dispersed in distilled H_2O (20 mL) in a round bottom flask that contains a magnetic stir bar. This blend was heated to 60 °C under stirring (400 rpm) until this temperature was reached. After that, 5 mL of NaOH (0.05 M) were added and after one minute, oleic acid, OA (0.6 mL), was also added. This blend remained at 60 °C for 30 min and then temperature is increased to 95 °C and was refluxed for 1 h 30 min, observing aggregation. The excess of NaOH was neutralized using HCl and the formed precipitate (TiO_2-OA) was isolated by centrifugation under 4000 rpm for 10 min and washed two times with ultrapure water and hexane. Subsequently, the obtained nanodispersion (hexane with TiO_2 nanoparticles coated with OA) was added to PAO8 using an ultrasonic bath to homogenize the new dispersion. Finally, a hot plate was used to evaporate the hexane (low boiling point) thus obtaining the desired PAO8 + TiO_2-OA nanolubricant (3 wt% in TiO_2-OA). Fig. 2 presents the preparation scheme of the nanodispersions of TiO_2-OA nanoparticles in PAO8.

To confirm that the OA coating is properly linked to the TiO_2 nanopowders, FTIR analyses of synthetized TiO_2-OA nanopowders were carried out with a spectrometer VARIAN 670-IR. Fig. 3 provides the FTIR spectrum of OA, TiO_2 and coated TiO_2-OA nanoparticles. The peaks at 2910 and 2846 cm^{-1} for the TiO_2-OA nanoparticles evidence that CH_3 and CH_2 of OA are present in the coated TiO_2 molecular structure [18]. Furthermore, peaks at 1490 and 1452 cm^{-1} prove that the –COO – functional group of OA is present [18]. In this regard, the disappearance of the intense peak at 1708 cm^{-1} implies that the –COOH of OA has totally reacted with TiO_2 nanoparticles to form the coated TiO_2-OA nanopowders [18]. Furthermore, an absorption band for the nano-TiO_2 core is identified at low frequencies, because of the peak around 540 cm^{-1} is associated to the Ti—O—O bond vibration [19]. Considering these FTIR results, it is confirmed that the OA coating was carried out successfully. Bare TiO_2 nanoparticles were also characterized by means of scanning electron microscopy (SEM) to obtain information about its shape. Fig. 4 shows the TiO_2 nanoparticles with two magnifications observing that these nanoparticles have roughly spherical spongy shape.

2.2. Formulation of nanodispersions

Nanolubricants were prepared with various weight percentages of TiO_2-OA (0.10, 0.25, 0.35 and 0.50 wt%) in PAO8. To prepare these nanodispersions, dilutions of the previously obtained 3 wt% TiO_2-OA nanolubricant were carried out adding PAO8. Furthermore, to improve the dispersibility of nanoparticles in the PAO8 oil, oleic acid was added for each TiO_2-OA nanodispersion to obtain an OA mass concentration of 0.2 wt%. Finally, the nanodispersions were homogenized by means of an ultrasonic bath (Fisherbrand FB11203), operating in continuous sonication mode (4 h, 180 W and 37 kHz). It should be noted that during the sonication procedure the temperature was under control to prevent overheating

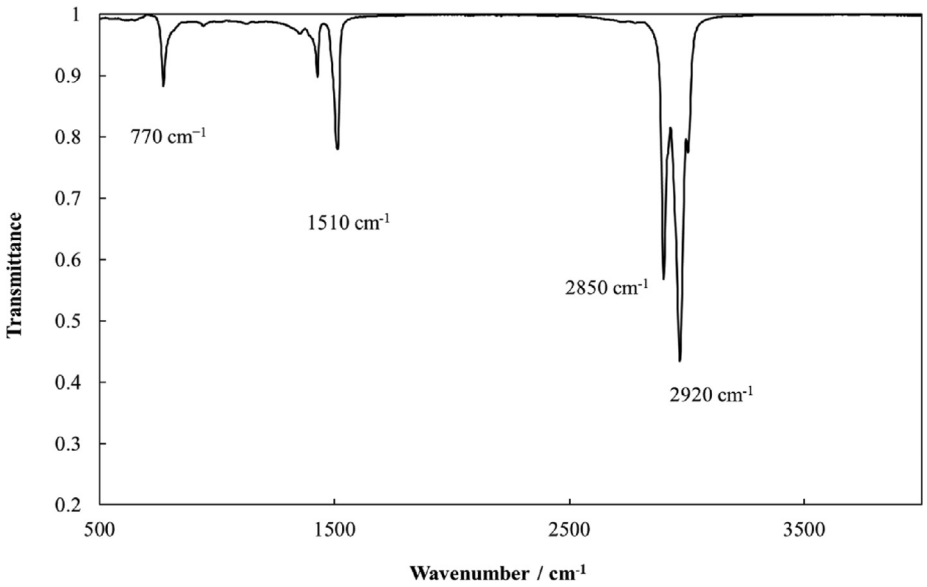

Fig. 1. FTIR spectrum of PAO8 base oil.

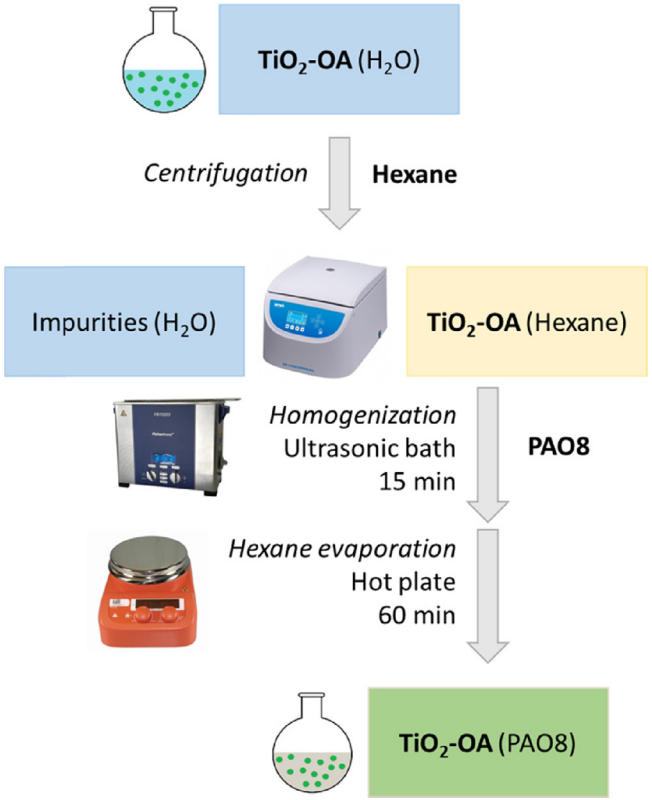

Fig. 2. Preparation scheme of the nanodispersions of TiO_2-OA nanoparticles in PAO8.

of samples. Furthermore, nanodispersions stability was examined by sediment photo capturing of lubricants and by measuring the evolution of the refractive index during time by means of a Mettler Toledo refractometer.

2.3. Thermal conductivity of lubricants

Thermal conductivities of PAO8 base oil and the optimal TiO_2-OA nanolubricant (0.35 wt%) were measured at 20 °C, 30 °C, 40 °C and 50 °C using a Tempos thermal properties analyzer (METER Group, USA). This device is based on the principle of the transient hot wire method [20]. This analyzer was used together with a KS-3 sensor, which consists of a single-needle (60 mm length and 1.3 mm diameter) with a heating element and a temperature sensor inside. The accuracy of thermal conductivity measurements is around 10 % in the range (0.02–2.00) $W{\cdot}m^{-1}{\cdot}K^{-1}$. A lubricant volume of around 30 mL is introduced in a sealed glass vial. The probe (needle) is placed in the middle of the vial. Subsequently, the vial is fully submerged and vertically placed in a temperature-controlled water bath. Measurements have been performed in low-power mode, which helps to prevent free convection in liquid samples. Five replicates of thermal conductivity measurements were performed for each temperature. Verification of the sensor was achieved by measuring pure glycerin, which is a thermal conductivity standard.

2.4. Tribological tests

2.4.1. Pure sliding conditions

Friction tests were performed at pure sliding conditions with a MCR 302 rheometer from Anton-Paar provided with a tribology cell *T*-PTD 200, using a H-PTD 200 Peltier hood for an accurate control of temperature. In this work, ball-on-three-pins test configuration was used. In this setup, the ball is placed on a shaft and is set to rotate by the rheometer motor, while is pressed against the pins. The axial force of the rheometer (in this case 20 N) is transmitted into a normal force acting vertical to the contact points on each pin (9.43 N resulting in a maximum contact pressure of approximately 0.8 GPa). Tests were made at a rotational speed of 213 rpm during 3400 s at 120 °C. The ball has 12.7 mm diameter and a roughness of 0.02 μm, while the pins have sizes of 6 mm in diameter and height and a roughness of 0.05 μm. Both specimens are made of hardened 100Cr6 steel and have a hardness of 62–66 Rockwell C. Pins and balls were washed with hexane prior to the tribological tests. Pins were fully flooded by adding around 1.2 mL of each tested lubricant. To achieve representative values, at least 3 replicates were performed with each nanolubricant. More details about this device can be found in previous articles [21–25]. With the aim of analyzing the worn surface after tribological tests, a 3D Optical Profilometer was utilized to measure the wear produced on the pins.

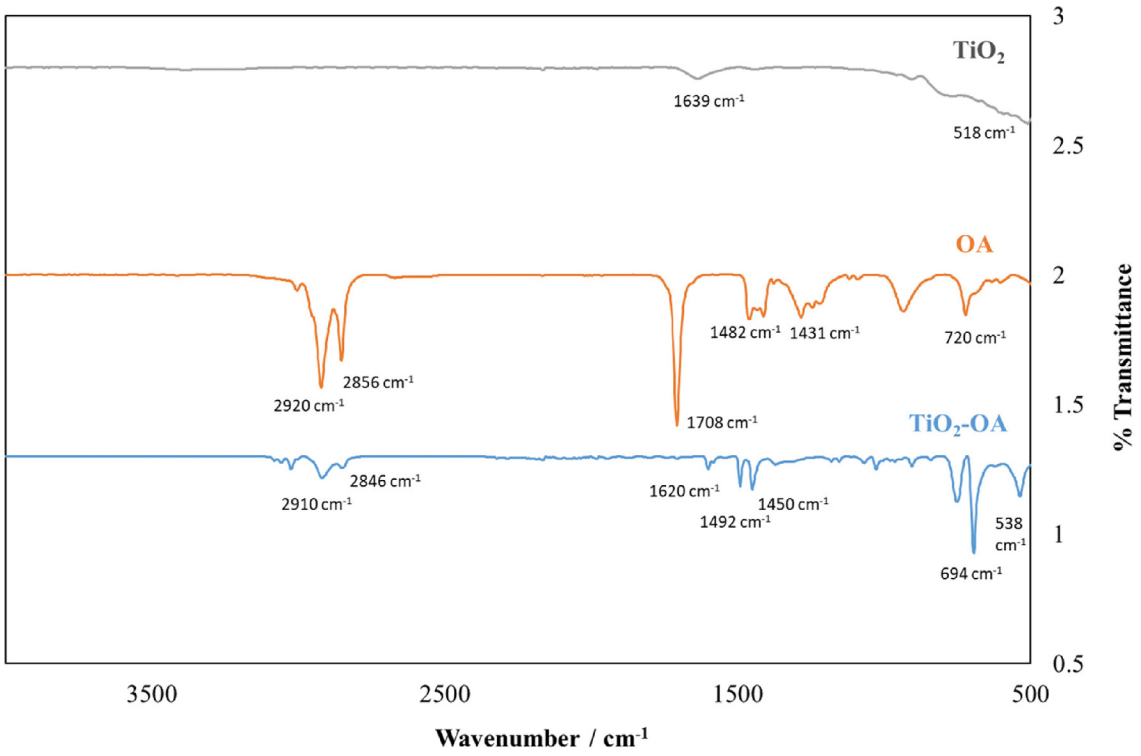

Fig. 3. FTIR spectrum of TiO_2 nanoparticles, OA, and coated TiO_2-OA nanoparticles with their characteristic vibrational bands.

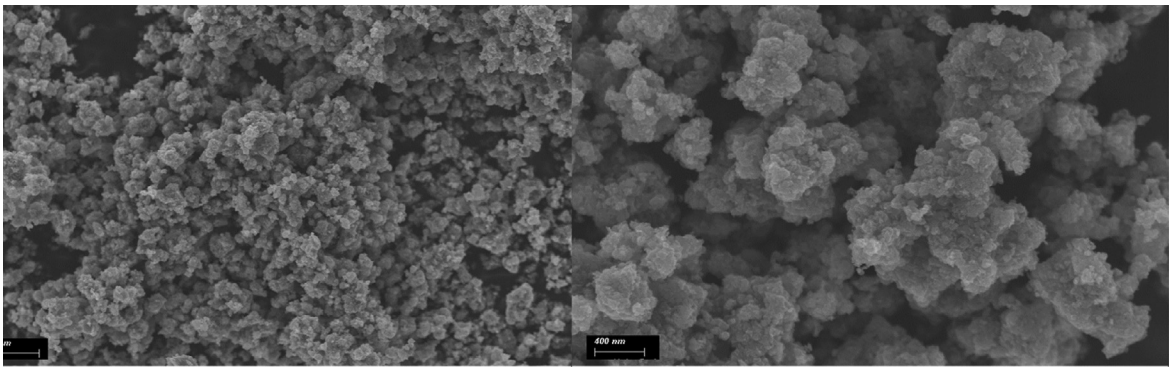

Fig. 4. SEM images of TiO_2 nanopowders.

Wear scar diameter (WSD), wear track depth (WTD) and worn area were the three wear parameters evaluated in the three pins in a confocal mode with a 10X objective. Furthermore, the roughness (Ra) of worn pins were also measured with the same 3D profiler to identify the tribological mechanisms due to the modified nanoparticles as additives to PAO8. The roughness was evaluated according to ISO4287 standard utilizing a Gaussian filter with a cut-off of 0.08 mm. With the aim of obtaining information about the distribution of nanoparticles and oil on the worn pins, a WITec alpha300R+ confocal Raman microscope at 532 nm was utilized. Prior to the Raman analyses, the worn surfaces were cleaned with hexane.

2.4.2. Rolling-sliding conditions: Stribeck curves

A ball-on-disc tribometer, EHD2, from PCS Instruments (London, UK) was used to determine the friction behavior of a contact pair consisting of a carbon chrome steel ball with a 19.05 mm diameter and a rotating carbon chrome steel disc. Disc and ball are run with two electric motors to perform the tests in rolling-sliding motion. The selected normal load is automatically applied with a load cell. The friction force is determined on the ball by means of a torque cell installed on the ball shaft, firstly when the disc is rotating quicker than the ball, and then, for the identical entrainment speed when the ball turning faster than disc. Subsequently, coefficient of friction is determined with normal force and friction forces. More information about this tribometer can be observed in previous articles [22,24]. It should be noted that these friction tests were performed for the PAO8 base oil and the TiO_2-OA nanolubricants under fully flooded lubrication (around 130 mL of lubricant) at the operating temperature of 120 °C, under a constant 50 N load that generates a maximum Hertz pressure of 0.7 GPa, and a 5 % slide-to-roll ratio (SRR):

$$SRR(\%) = 2 \times \frac{(U_{disc} - U_{ball})}{(U_{disc} + U_{ball})} \times 100 \quad (1)$$

U_{disc} and U_{ball} are the speeds of the contact points of the disc and the ball respectively, whereas the entrainment speed (U_s) is:

$$U_S = \frac{(U_{disc} + U_{ball})}{2} \quad (2)$$

For the three discs (two rough and one smooth, Fig. 5) friction properties of TiO_2-OA nanolubricants and PAO8 base oil were analyzed by means of Stribeck curves for a 5 % SRR value. For each test, the same ramp of entrainment speed was used: 0.05 m/s to 2 m/s. Specifically, the lowest speed of ball is 0.047 m/s and the highest is 1.997 m/s for all the tests whereas, the lowest speed of disc is 0.052 m/s and the highest is 2.101 m/s. During tests, the EHD2 tribometer regulates automatically disc and ball speeds, being the speed of disc faster to reach positive SRR whereas the entrainment speed remains constant. The friction coefficient is obtained as the average of those achieved from two different friction tests, one ramp raising speed and the other one reducing speed. Ball and disc properties (Table 1) were supplied by the producer while the surface roughness of the ball and the three discs was measured with a Profiler Hommelwerke (Table 1).

3. Results

3.1. Stability of the nanolubricants

The temporal stability of TiO_2-OA nanolubricants against sedimentation was investigated through visual observation as well as with refractometry. Fig. 6 evidence that for the four designed TiO_2-OA nanolubricants no signs of sedimentation have appeared for at least three weeks just after homogenization. Nevertheless, for the most concentrated (and less stable) TiO_2-OA nanolubricant (0.50 wt%), it seems that sedimentation starts to occur at 4 weeks after sonication. It should be noted that the visual stability of uncoated TiO_2 nanolubricants was<48 h (Fig. 7), therefore an important stability improvement was achieved with the OA coating. Thus, the stability time of prepared TiO_2-OA nanolubricants is much greater than that required to carried out pure sliding and rolling-sliding tribological tests, around 8 h.

The other method used to test the temporal stability of TiO_2-OA nanolubricants against sedimentation is refractometry. Fig. 8 presents the time evolution of the refractive index for the TiO_2-OA nanolubricant and for the bare TiO_2 nanolubricant, both with a NP concentration of 0.10 wt%. It can be clearly observed that for the 0.10 wt% TiO_2 nanolubricant after the first ten hours the nanoparticles are full sedimented, whereas in the case of the 0.10 wt% TiO_2-OA nanolubricant the sedimentation is slower. Specifically, for the former nanolubricant the refractive index increased 0.27 % after 10 h while for the TiO_2-OA nanolubricant it raised just 0.06 %, which indicates that the oleic acid coating of TiO_2 nanoparticles clearly enhances the stability of nanolubricants. Moreover, the TiO_2-OA refractive index evolution shows a significant enhancement in the stability compared to other earlier measured nanolubricants [25]. In particular, with trimethylolpropane trioleate based nanolubricants (higher viscosity oil) containing graphene oxide nanoadditives, refractive index raises 0.44 % after 50 h [25], whereas for the same time (50 h) and with a very low viscosity oil, the refractive index evolution shows increases of 0.32 % for 0.10 wt% TiO_2-OA nanolubricant. It should be noted that for low viscosity oils is more difficult to find good stabilities, since the nanoparticles have less resistance to drop in oil. Considering this fact, in this research a great stability was achieved owing to the coating with oleic acid of the TiO_2 nanoparticles.

3.2. Thermal conductivity results

Experimental thermal conductivity measurements of PAO8 base oil and 0.35 wt% TiO_2-OA nanolubricant are shown in Fig. 9 from 20 °C to 50 °C. The measurements indicate that for both lubricants the thermal conductivity values remains almost constant when the temperature rises (Fig. 9). The 0.35 wt% TiO_2-OA nanolubricant has approximately the same thermal conductivity values than PAO8 being around 0.15–0.16 W/m K at all the evaluated temperatures.

3.3. Friction results of pure sliding tests

Mean friction coefficients (μ) obtained under pure sliding conditions for PAO8 and the four nanolubricants composed by

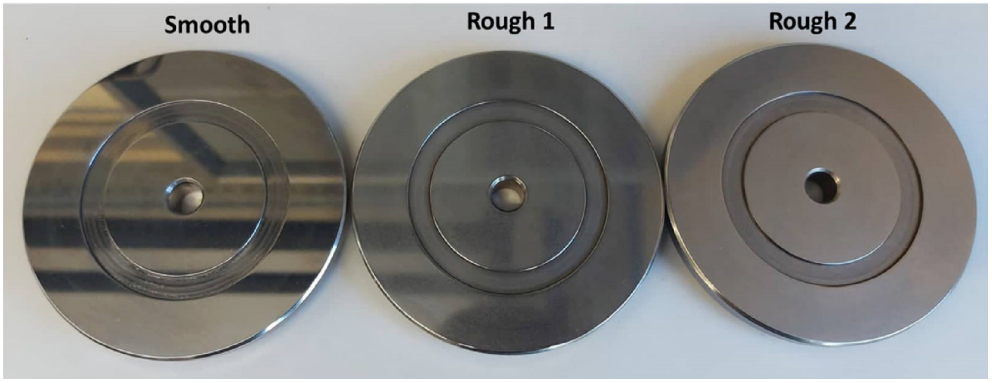

Fig. 5. Smooth and rough discs used in rolling-sliding tribological tests.

Table 1
Main physical characteristics of ball and discs used in rolling-sliding tribological tests.

Parameters	Steel Ball	Steel Discs		
		Smooth	Rough 1	Rough 2
Elastic modulus / GPa	210	210	210	210
Poisson coefficient	0.29	0.29	0.29	0.29
Diameter / mm	19.05	100	100	100
Surface roughness, Ra / nm	20	20	100	340
Hardness (Rockwell C)	62–66	62–66	62–66	62–66

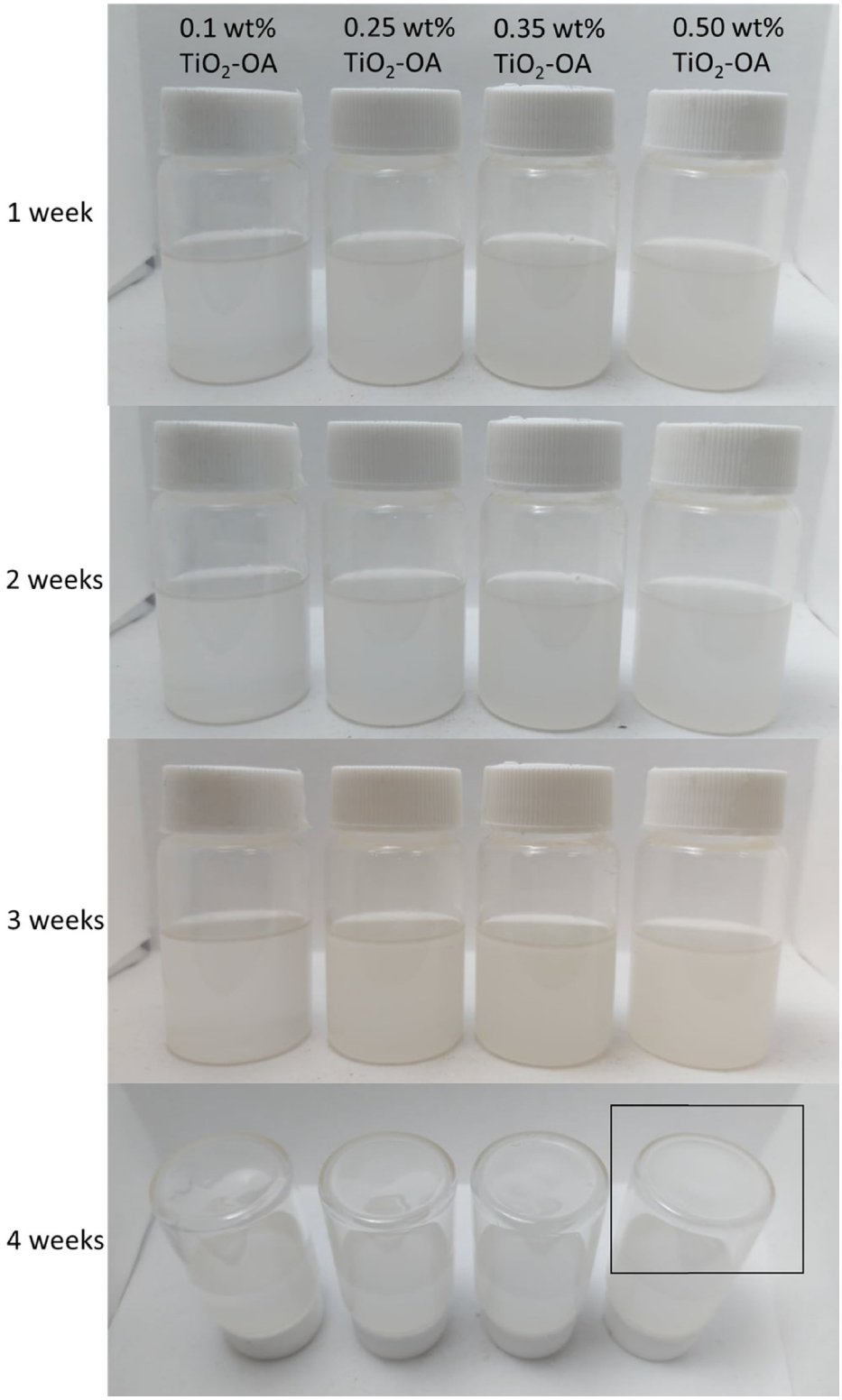

Fig. 6. Visual stability of TiO_2-OA nanolubricants.

TiO_2-OA with PAO8 base oil are presented in Fig. 10 and Table 2. It can be obviously seen that for the all TiO_2-OA nanolubricants the achieved coefficients of friction are lower than that of PAO8 without additives, being the greatest friction decrease achieved for the nanolubricant containing 0.35 wt% TiO_2-OA nanoparticles. Specifically, the lowest average coefficient of friction is 0.098, obtained with this last nanolubricant, whereas the one obtained for the base oil is 0.139. Thus, a maximum 30 % friction reduction owing to the TiO_2-OA nanoadditives is achieved. Regarding the other nanolubricants, friction reductions of 16 %, 24 % and 23 % were obtained for 0.10 wt% TiO_2-OA, 0.25 wt% TiO_2-OA and 0.50 wt% TiO_2-OA nanolubricants, respectively.

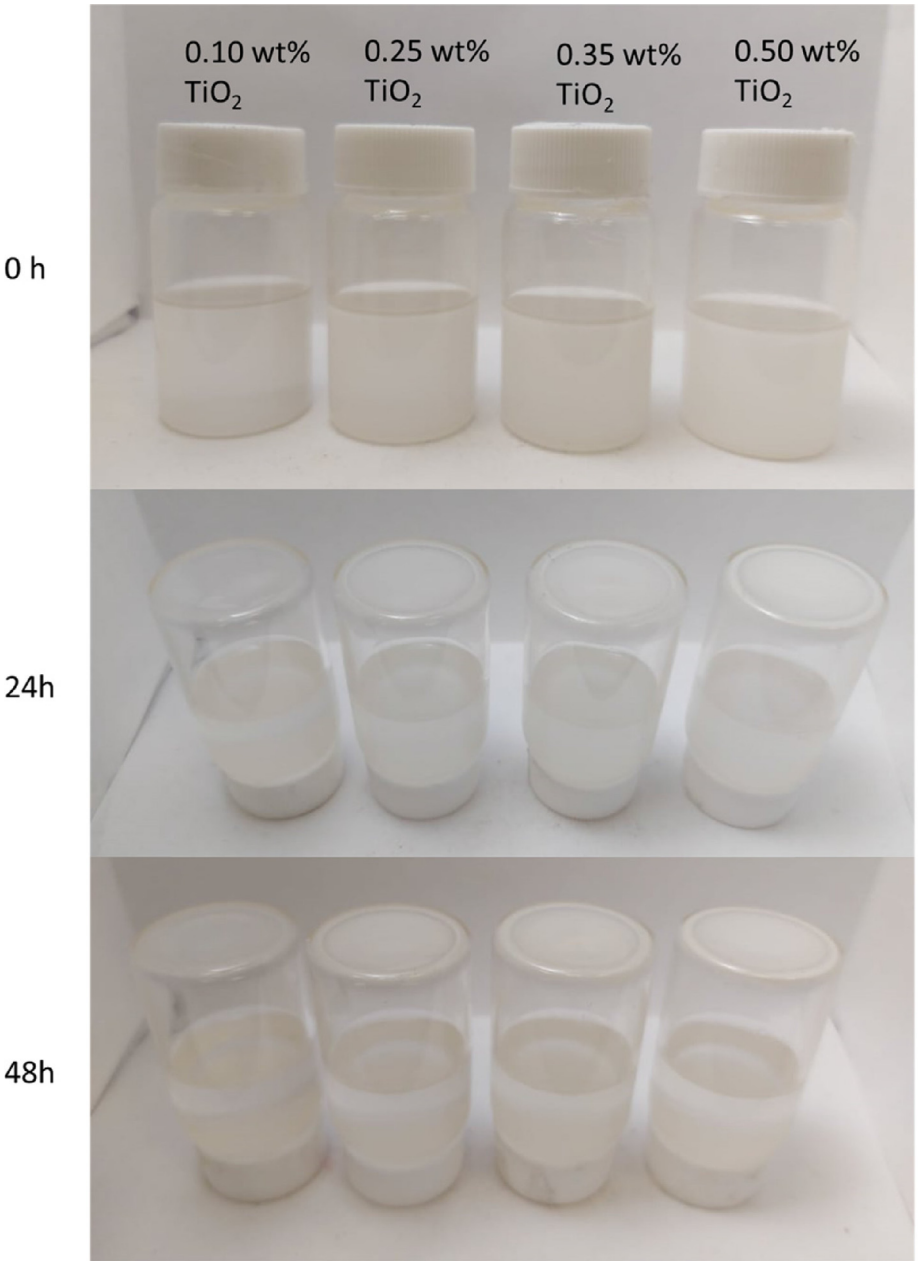

Fig. 7. Visual stability of uncoated TiO_2 nanolubricants.

3.4. Surface analysis of worn pins

To compare qualitatively 3D Profiles, worn areas and cross section profiles of the pins tested with the PAO8 base oil and with the optimal TiO_2-OA nanolubricant for pure sliding tests are shown in Figs. 11 and 12. Average wear produced in pins after tribological tests was quantified by means of different parameters: WSD, WTD and worn area, which results are reported in Table 2 for each lubricant tested. As it can be observed, for all the tested TiO_2-OA nanolubricants, the three wear parameters were smaller than those found with PAO8 oil. The maximum wear reductions were found for 0.35 wt% TiO_2-OA nanolubricant with reductions of 26 %, 65 % and 73 % for WSD, WTD and worn area, respectively. These impressive wear reductions can be clearly observed in Figs. 10 and 11 for the nanolubricant with the optimal concentration (0.35 wt% TiO_2-OA). Wear results show a good correlation with friction, as it can be observed in Fig. 10.

Furthermore, roughness (Ra) of worn tracks of pins was investigated to obtain more information about the antiwear properties of TiO_2-OA nanoparticles. Worn tracks lubricated with TiO_2-OA nanolubricants are less rough than those lubricated with PAO8 without additives (Table 3). In particular, a Ra value of 18.8 nm was found for the worn track lubricated with PAO8 while for the surface lubricated with the 0.35 wt% TiO_2-OA nanolubricant a smaller Ra was reached (12.8 nm), which leads to a 32 % roughness reduction. Therefore, it can be suggested that polishing and/or mending effects occur owing to the presence of TiO_2-OA nanopowders. Due to the mending effect, nanoparticles can fill the grooves and scars of the rubbing surface developing an improved surface finish [26,27]. To quantify better the effect of the TiO_2-OA nanoparticles in the roughness, other two parameters were analyzed: skewness, Rsk, and kurtosis, Rku. The untested surface has a Rsk higher than 0 (1.51), which means that the surface contains more peaks and asperities than valleys [28]. The decrease in the Rsk

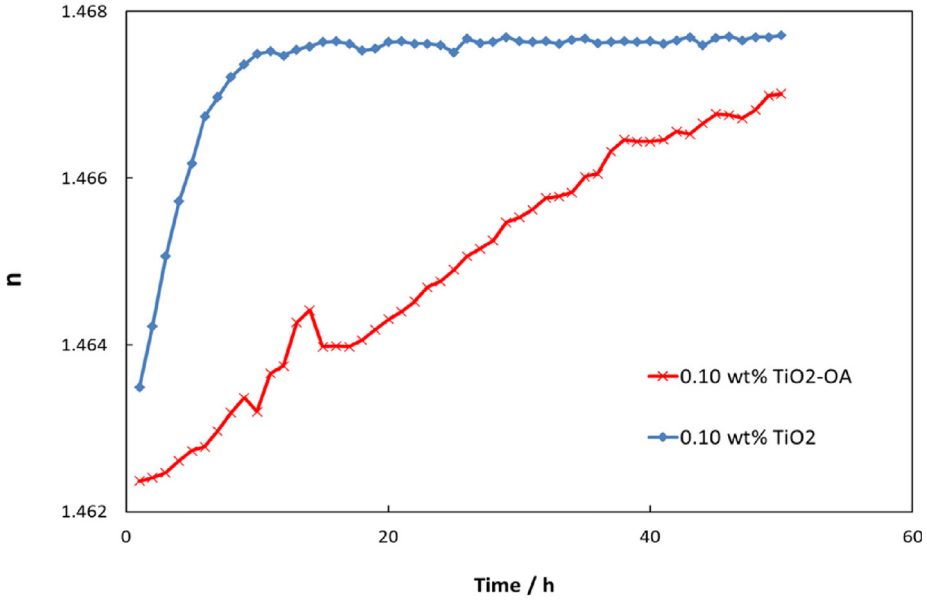

Fig. 8. Refractive index evolution for 0.10 wt% TiO_2 and TiO_2-OA nanolubricants.

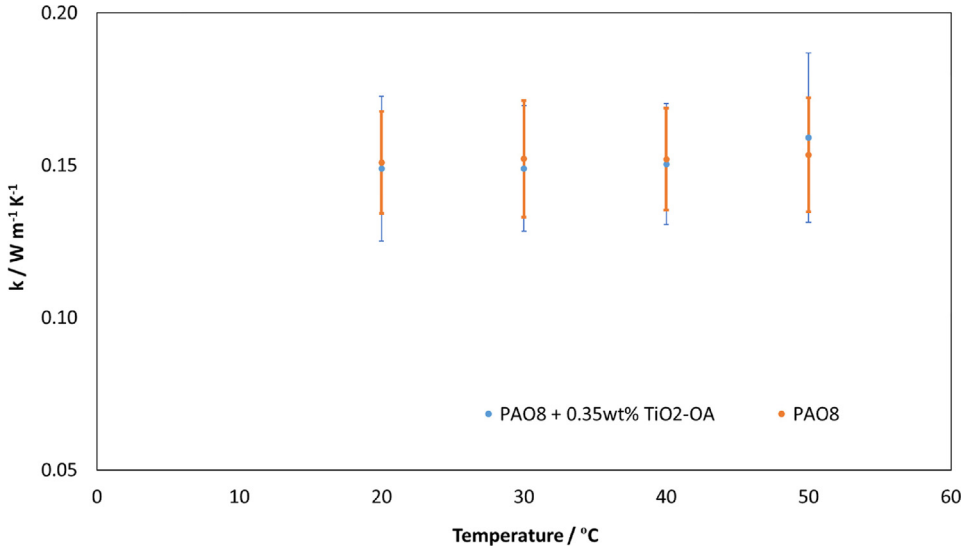

Fig. 9. Effect of temperature on thermal conductivity of PAO8 base oil and 0.35 wt% TiO_2-OA nanolubricant.

parameter due to the friction process to a negative value closer to zero (-0.76 – -0.35) confirms that the worn surfaces lubricated with base oil and nanolubricants are very flat, most of the material being concentrated around the valleys. As regards Rku, the value before tribological tests is higher than 3 (5.54), which indicates the presence of very high peaks and/or deep valleys (this parameter does not distinguish between peaks and valleys) [28]. After friction tests this value decreases (2.98–2.41), which implies low both peaks and valleys. Comparing the mean Ra, Rsk and Rku values of the worn pins lubricated with PAO8 with those of worn pins lubricated with PAO8 + 0.35 wt% TiO_2-OA, it can be concluded that the last pins have flatter worn surfaces. These facts confirm that polishing and/or mending effects takes place. Table 3 also shows that the worn surfaces lubricated with PAO8 + 0.5 wt% TiO_2-OA are flatter than those tested with the optimal nanolubricant (PAO8 + 0.3 5 wt% TiO_2-OA).

Finally, with the aim of obtaining information about the nanoparticle distribution in worn tracks after pure sliding tests, Raman mappings of the worn surfaces were recorded. First, Raman spectra of the PAO8 base oil (Fig. S1), oleic acid (Fig. S2) and the TiO_2 nanopowders (Fig. S3) were obtained to identify the components in mapping. Therefore, mapping of the worn pin lubricated with the optimal TiO_2-OA nanolubricant (Fig. 13) was performed to identify the role that nanoparticles play in the wear decrease. Fig. 13 shows the relevant areas in green and blue color, that coincide with the spectra obtained for TiO_2 and OA, Figs. S3 and S4, respectively. This fact indicates that tribofilms containing OA and TiO_2 were produced on the worn surface during the friction test. Considering the Raman and roughness results, it seems that the main tribological mechanisms that occur are tribofilm formation, mending and polishing.

3.5. Rolling-sliding tribological results: Stribeck curves

Rolling-sliding tribological measurements for PAO8 base oil and the designed TiO_2-OA nanolubricants were carried out at the same

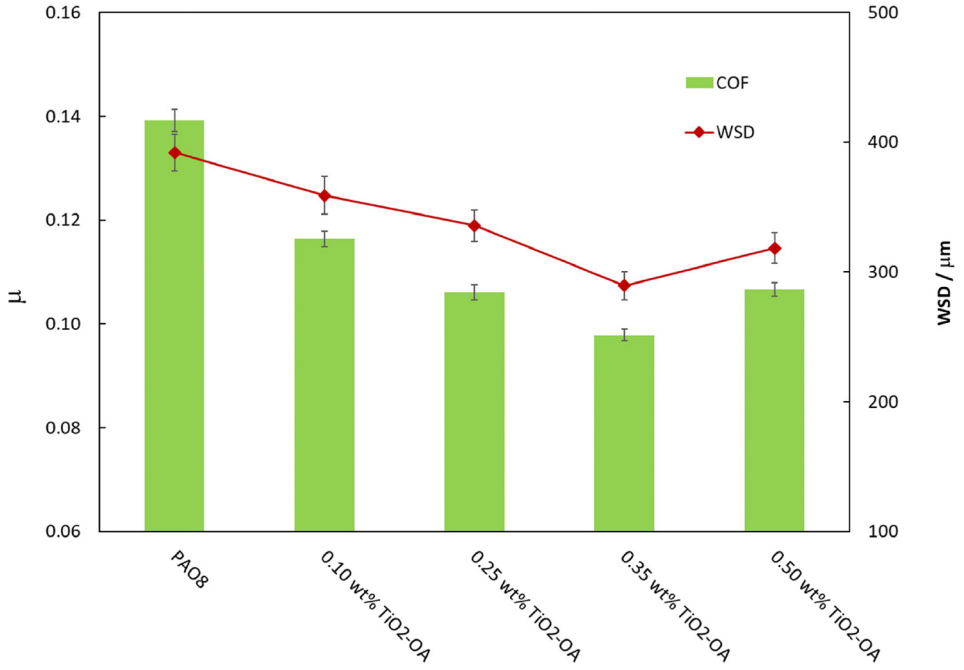

Fig. 10. Mean friction coefficient, μ, and WSD with PAO8 and its nanolubricants containing TiO_2 nanoparticles coated with oleic acid.

Table 2
Mean coefficients of friction, μ, and mean wear parameters, including their standard deviations, for the tested PAO8 lubricants.

Lubricant	μ	σ	WSD/μm	σ/μm	WTD/μm	σ/μm	Area/ μm²	σ/ μm²
PAO8	0.139	0.002	392	14	2.35	0.17	605	52
+ 0.10 wt% TiO_2-OA	0.116	0.002	359	14	2.11	0.18	527	41
+ 0.25 wt% TiO_2-OA	0.106	0.002	336	12	1.85	0.12	459	39
+ 0.35 wt% TiO_2-OA	0.098	0.001	289	11	0.82	0.11	163	18
+ 0.50 wt% TiO_2-OA	0.107	0.001	318	12	1.04	0.14	245	17

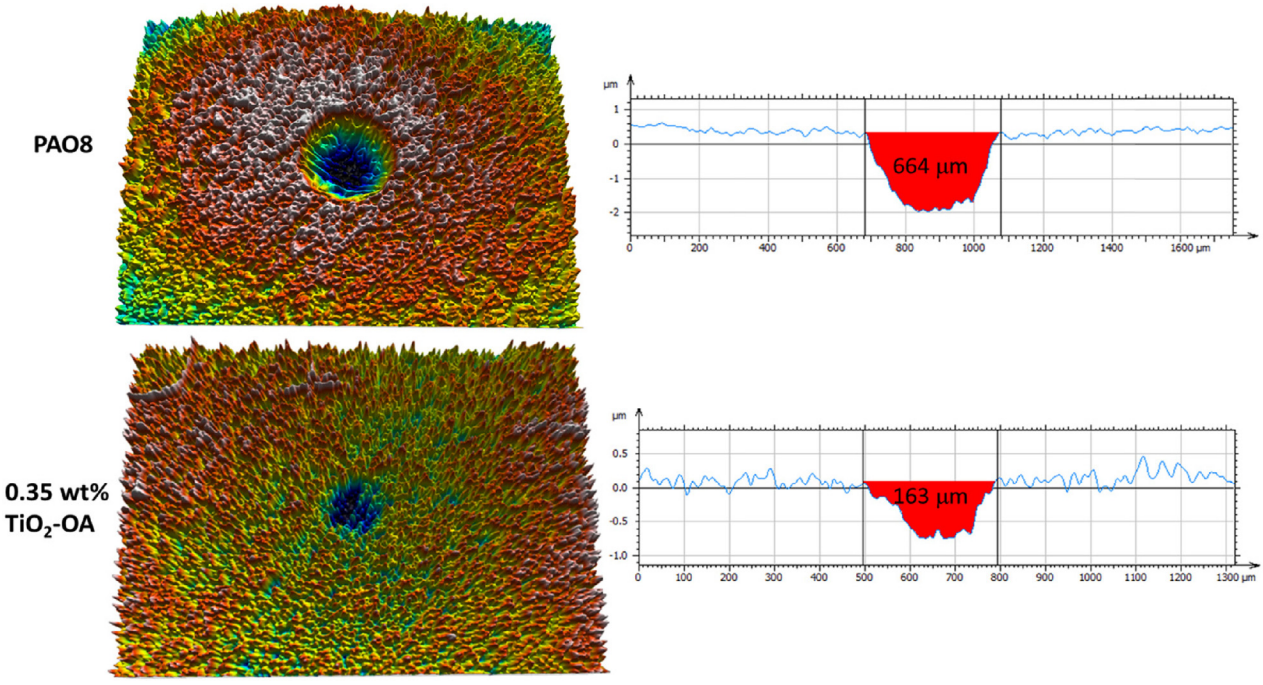

Fig. 11. 3D images and worn areas of worn tracks lubricated with PAO8 oil and with the optimum TiO_2-OA nanolubricant (0.35 wt%).

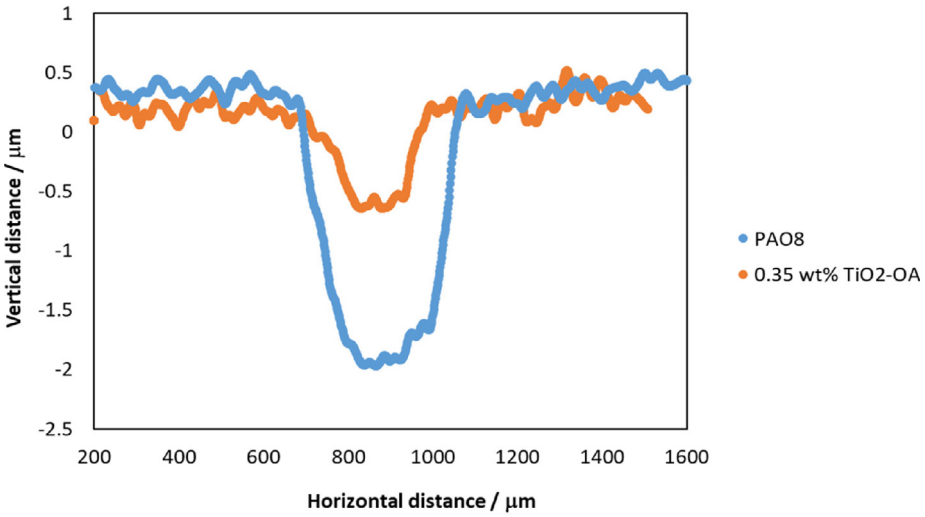

Fig. 12. Profiles comparison of worn tracks lubricated with PAO8 oil and with the 0.35 wt% TiO_2-OA nanolubricant.

Table 3
Mean roughness parameters, Ra, Rsk and Rku and their uncertainties, σ, in worn pins tested with PAO8 lubricants (Gaussian filter: 0.08 mm cut-off).

Lubricant	Ra/nm	σ	Rsk	σ	Rku	σ
PAO8 base oil	18.8	1.7	−0.562	0.048	2.98	0.21
+ 0.15 wt% TiO_2-OA	15.7	1.5	−0.434	0.055	2.44	0.18
+ 0.25 wt% TiO_2-OA	14.4	1.7	−0.512	0.045	2.41	0.17
+ 0.35 wt% TiO_2-OA	12.8	1.2	−0.356	0.052	2.46	0.18
+ 0.50 wt% TiO_2-OA	13.3	1.1	−0.762	0.062	2.52	0.15

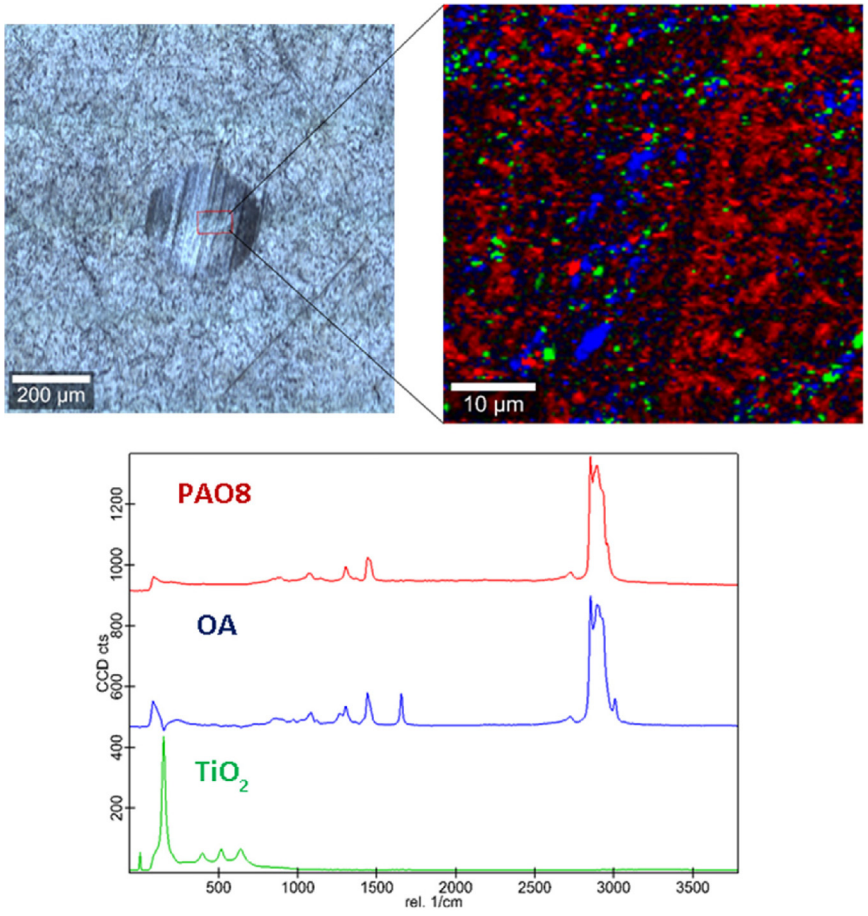

Fig. 13. Elemental mapping and Raman characterization of worn surface obtained with the PAO8 + 0.35 wt% TiO_2-OA nanolubricant.

temperature than pure sliding tests (120 °C) and with a SRR of 5 %, by performing Stribeck Curves (Figs. 14 and 15). In this manuscript, these curves are presented plotting the coefficient of friction versus specific film thickness Λ that is defined by the following expression:

$$\Lambda = \frac{h_t}{Ra} \tag{3}$$

where h_t is the theoretical central film thickness and Ra is the composite average roughness of the surfaces given by $Ra = \sqrt{(Ra_{disc})^2 + (Ra_{ball})^2}$. The theoretical central film thickness (h_t) at the temperature of 120 °C was calculated by means of the Hamrock and Downson's equation [29], considering the geometry and material properties of ball and discs (roughness, Young's modulus and Poisson's ratio reported in Table 1), the lubricant properties (viscosity and pressure – viscosity coefficient) and the operating conditions (entrainment speed, load and SRR). It should be noted that for the theoretical central film thickness estimation, the pressure – viscosity coefficient of PAO6 was used [30]. Regarding the viscosities, a Stabinger SVM3000 from Anton Paar was used to measure them up to 100 °C (Table S1). The Vogel – Fulcher – Tammann equation [30] was utilized to correlate the experimental dynamic viscosities of each tested lubricant at atmospheric pressure, obtaining the dynamic viscosity of each nanolubricant and the base oil at 120 °C from this equation, since the viscosimeter does not allow the measurement of viscosity above 100 °C.

Stribeck curves are presented in Figs. 14 and 15 for PAO8 base oil and TiO_2-OA nanolubricants with the three different discs (Table 1). As usual, friction tests carried out with the rough discs showed higher friction values than those made with the smooth disc. Fig. 12 clearly shows that, for each tested disc, the friction coefficients are quite lower for all the TiO_2-OA nanolubricants than for the PAO8 base oil. Once again, the best friction behavior was found for the 0.35 wt% TiO_2-OA nanolubricant and that is why only the full Stribeck curves of PAO8 base oil and 0.35 wt% TiO_2-OA nanolubricant are presented in Fig. 15. The results presented in

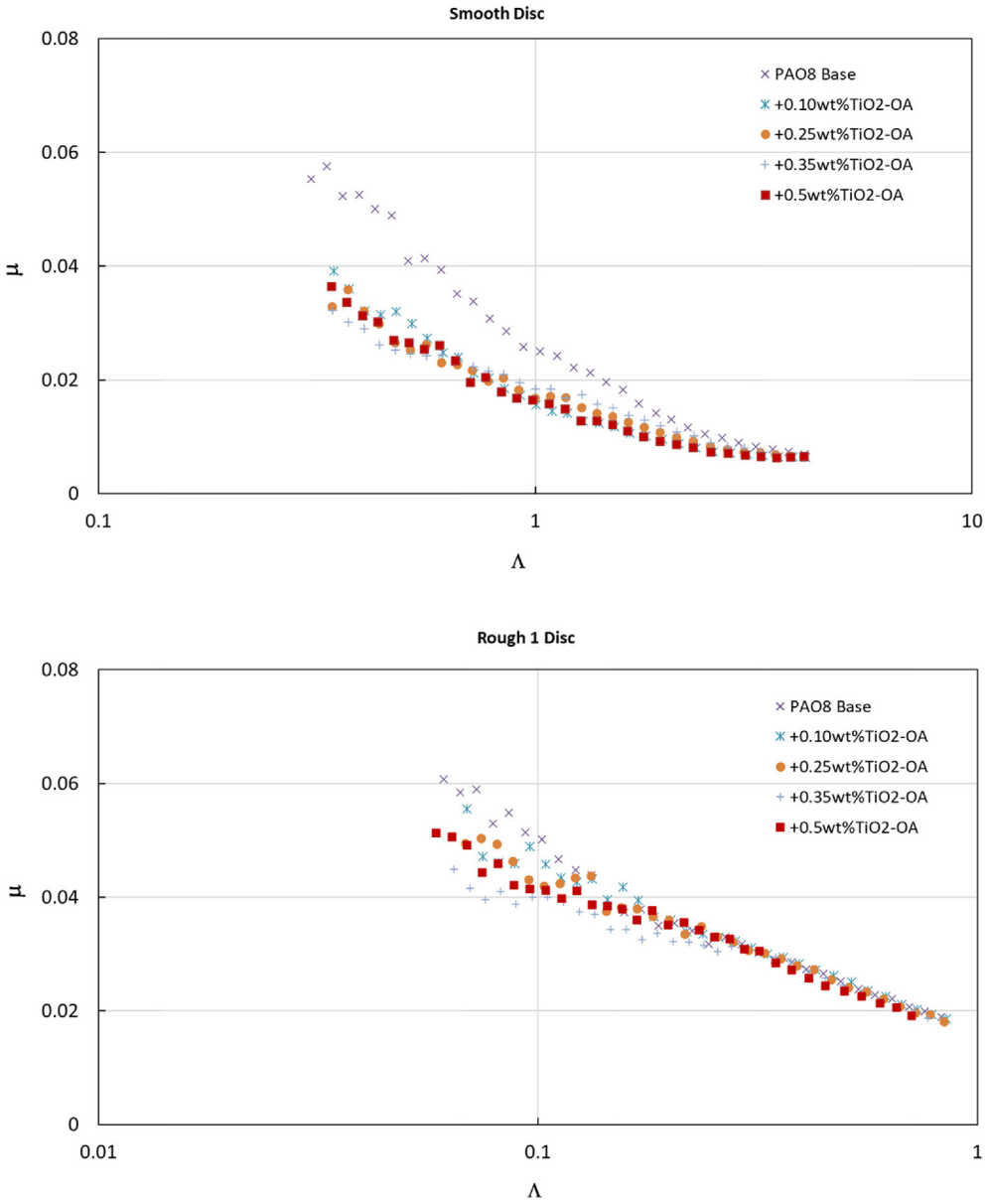

Fig. 14. Stribeck curves of PAO8 and PAO8 + TiO_2-OA nanolubricants tested with each disc at 120 °C and 5 % SRR.

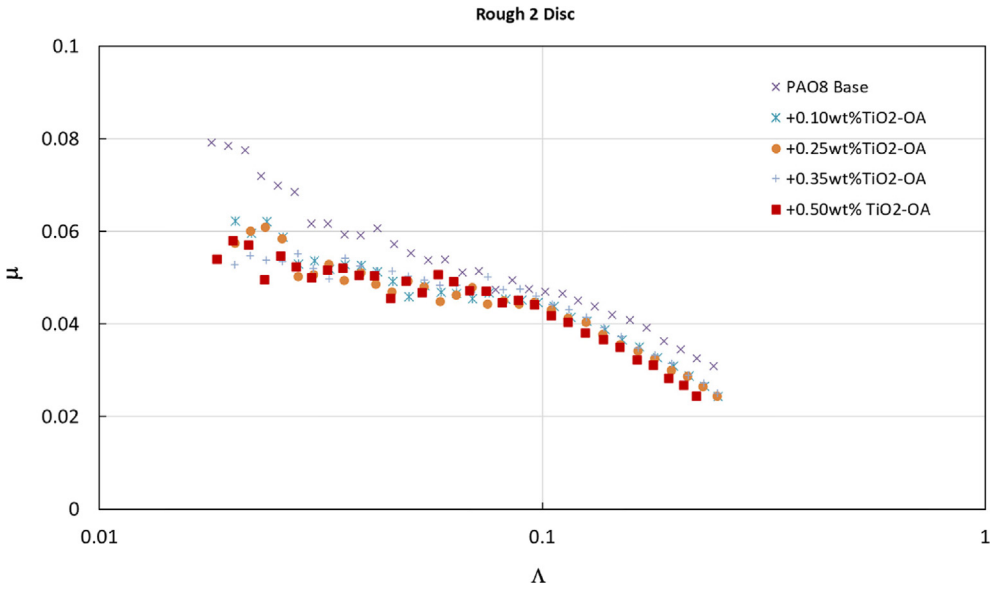

Fig. 14 (*continued*)

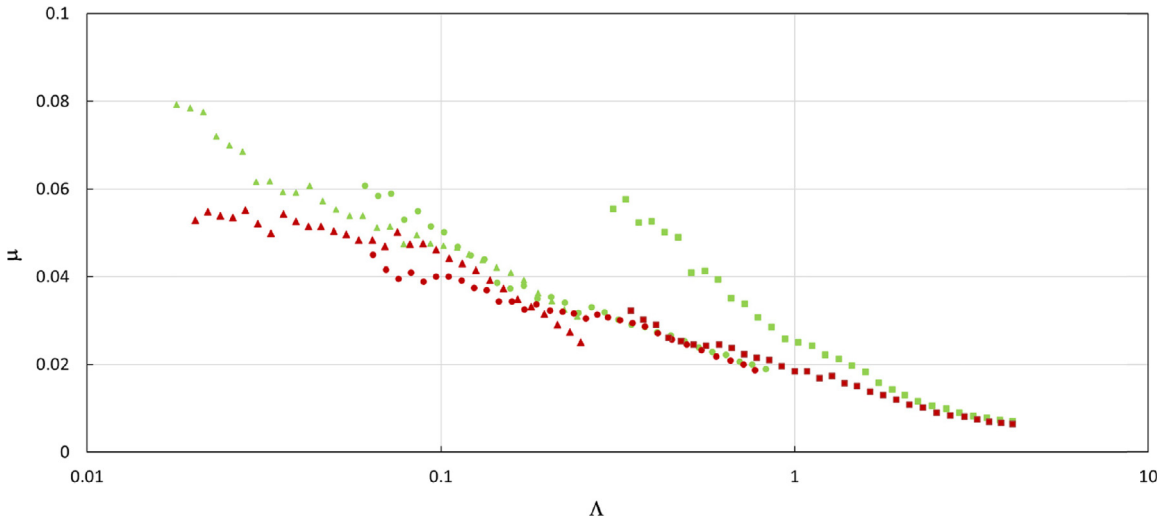

Fig. 15. Full Stribeck curves of PAO8 (green) and PAO8 + 0.35 wt% TiO_2-OA nanolubricant (red) tested with each disc (squares smooth, circles rough 1, triangles rough 2) at 120 °C and 5 % SRR. (For interpretation of the references to color in this figure legend, the reader is referred to the web version of this article.)

Fig. 14 for each disc are very interesting since it can be observed that for high entrainment speeds (right part of the curves) and consequently higher specific film thickness, the friction coefficient is quite similar for all nanolubricants and base oil. However, at low entrainment speeds the effect of TiO_2-OA nanoparticles is crucial, contributing to greatly reduce the friction when the hydrodynamic effect is poor (low speeds). Regarding the effect of nanoparticles concentration in friction behavior, the friction coefficient decreases as the concentration of nanoparticles increases, until the optimal value of 0.35 wt% is reached. This result is in perfect agreement with the friction results obtained for the pure sliding tests, where the 0.35 wt% TiO_2-OA concentration was also the optimal ones. A higher nanoparticle content leads to higher friction values, which means that there should be a saturation point (optimal concentration) above which the nanoparticle content cannot provide further friction reduction.

In general, a full Stribeck curve is separated in four lubrication regimes: boundary, mixed, elastohydrodynamic and hydrodynamic and full film lubrication. Some authors [31–37] think that boundary lubrication happens if $\Lambda < 1$, mixed lubrication if $1 < \Lambda < 3$, elastohydrodynamic lubrication (EHL) when $\Lambda > 3$ and with $\Lambda > 5$, full film lubrication. According to the results shown in Fig. 14, the Λ ratios range between a minimum at about 0.02 (the roughest disc) to>6 (the smoothest disc). Hence, based on the previous articles [31–37] boundary film lubrication should occur for all the tested discs, whereas mixed and full film lubrication just occur for the smoothest disc at high speeds.

4. Conclusions

Four nanolubricants based on a low-viscosity oil, PAO8, and TiO_2-OA nanoparticles as antifriction and antiwear additives, and oleic acid as dispersant were tribologically characterized. The conclusions of this work can be brief as:

-Friction coefficients attained with TiO_2-OA nanolubricants are smaller than those observed for the neat PAO8 oil for all tribological tests (pure sliding or rolling/sliding contacts).

-In pure sliding conditions, for all the TiO_2-OA nanolubricants the wear observed in pins is much lower than the wear found for the PAO8 base oil with the best reductions reaching 26 %, 65 % and 73 % in width, depth, and area respectively (PAO8 + 0.35 wt% TiO_2-OA nanolubricant).

-From roughness measurements and Raman mappings of worn pins tested in pure sliding conditions, it is concluded that the lubrication mechanism can be described by the adsorbed tribofilm as well as the polishing and mending effects.

-In the rolling/sliding tests (small slide to roll-ratio SRR), the antifriction capability of TiO_2-OA nanoparticles is more important at low speeds, which shows that the use of nanoparticles is particularly important when operating in the boundary lubrication regime.

CRediT authorship contribution statement

José M. Liñeira del Río: Writing – original draft, Writing – review & editing, Methodology, Investigation, Conceptualization. **Fátima Mariño:** Writing – review & editing, Methodology, Investigation, Conceptualization. **Enriqueta R. López:** Writing – review & editing, Validation, Supervision, Formal analysis, Conceptualization. **David E.P. Gonçalves:** Writing – review & editing, Methodology, Validation, Supervision, Formal analysis. **Jorge H.O. Seabra:** Writing – review & editing, Project administration, Funding acquisition. **Josefa Fernández:** Writing – review & editing, Validation, Supervision, Project administration, Funding acquisition, Conceptualization.

Data availability

No data was used for the research described in the article.

Declaration of Competing Interest

The authors declare that they have no known competing financial interests or personal relationships that could have appeared to influence the work reported in this paper.

Acknowledgments

This research is supported by Xunta de Galicia (ED431C 2020/10), by MCIN/AEI/10.13039/501100011033 through the PID2020-112846RB-C22 project and by LAETA, Portugal under project UID/50022/2020. JMLDR is grateful for financial support through the Margarita Salas programme, funded by MCIN/AEI/10.13039/501100011033 and "NextGenerationEU/PRTR". FM acknowlegdes a IACOBUS grant to the European Grouping for Territorial Cooperation Galicia-Norte de Portugal (GNP-EGTC). Furthermore, authors also thank Repsol Lubricants for supplying us the PAO8 base oil and recognize the support of the RIAIDT-USC analytical skills.

Appendix A. Supplementary material

Supplementary data to this article can be found online at https://doi.org/10.1016/j.molliq.2022.121097.

References

[1] R. Shah, B. Gashi, A. Rosenkranz, Latest developments in designing advanced lubricants and greases for electric vehicles - an overview, Lubr. Sci. 34 (8) (2022) 515–526.
[2] W. Ahmed Abdalglil Mustafa, F. Dassenoy, M. Sarno, A. Senatore, A review on potentials and challenges of nanolubricants as promising lubricants for electric vehicles, Lubr. Sci. 34 (1) (2022) 1–29.
[3] L.I. Farfan-Cabrera, Tribology of electric vehicles: A review of critical components, current state and future improvement trends, Tribol. Int. 138 (2019) 473–486, https://doi.org/10.1016/j.triboint.2019.06.029.
[4] Lubes'n'Greases Perspective on Electric Vehicles Annual Report. LNG Publishing Company, Inc., 2019; 23–27.
[5] A. García, G.D. Valbuena, A. García-Tuero, A. Fernández-González, J.L. Viesca, A. H. Battez, Compatibility of Automatic Transmission Fluids with Structural Polymers Used in Electrified Transmissions, Appl. Sci. 12 (2022) 3608, https://doi.org/10.3390/app12073608.
[6] N. Rivera, J.L. Viesca, A. García, J.I. Prado, L. Lugo, A.H. Battez, Cooling Performance of Fresh and Aged Automatic Transmission Fluids for Hybrid Electric Vehicles, Appl. Sci. 12 (2022) 8911, https://doi.org/10.3390/app12178911.
[7] Y.-A. Kwak, C.S. Cleveland, A. Adhvaryu, X. Fang, S. Hurley, T. Adachi, Understanding Base Oils and Lubricants for Electric Drivetrain Applications, JSAE/SAE Powertrains, Fuels and Lubricants, 2019.
[8] M. Berly, Next Generation Driveline Lubricants for Electrified Vehicles, Tribology & Lubrication Technology 77 (2021) 38–40.
[9] S.C. Tung, M. Woydt, R. Shah, Global Insights on Future Trends of Hybrid/EV Driveline Lubrication and Thermal Management, Frontiers in Mechanical Engineering 6 (2020), https://doi.org/10.3389/fmech.2020.571786.
[10] W. Dai, B. Kheireddin, H. Gao, H. Liang, Roles of nanoparticles in oil lubrication, Tribol. Int. 102 (2016) 88–98, https://doi.org/10.1016/j.triboint.2016.05.020.
[11] G. Paul, S. Shit, H. Hirani, T. Kuila, N.C. Murmu, Tribological behavior of dodecylamine functionalized graphene nanosheets dispersed engine oil nanolubricants, Tribol. Int. 131 (2019) 605–619, https://doi.org/10.1016/j.triboint.2018.11.012.
[12] M.K.A. Ali, X. Hou, M.A.A. Abdelkareem, Anti-wear properties evaluation of frictional sliding interfaces in automobile engines lubricated by copper/graphene nanolubricants, Friction 8 (2020) 905–916, https://doi.org/10.1007/s40544-019-0308-0.
[13] M. Goodarzi, D. Toghraie, M. Reiszadeh, M. Afrand, Experimental evaluation of dynamic viscosity of ZnO–MWCNTs/engine oil hybrid nanolubricant based on changes in temperature and concentration, J. Therm. Anal. Calorim. 136 (2019) 513–525, https://doi.org/10.1007/s10973-018-7707-8.
[14] M. Kalin, J. Kogovšek, M. Remškar, Mechanisms and improvements in the friction and wear behavior using MoS_2 nanotubes as potential oil additives, Wear 280–281 (2012) 36–45, https://doi.org/10.1016/j.wear.2012.01.011.
[15] Y. Chen, P. Renner, H. Liang, Dispersion of Nanoparticles in Lubricating Oil: A Critical Review, Lubricants 7 (2019) 7, https://doi.org/10.3390/lubricants7010007.
[16] C. Birleanu, M. Pustan, M. Cioaza, A. Molea, F. Popa, G. Contiu, Effect of TiO_2 nanoparticles on the tribological properties of lubricating oil: an experimental investigation, Sci. Rep. 12 (2022) 5201, https://doi.org/10.1038/s41598-022-09245-2.
[17] V. Cortes, K. Sanchez, R. Gonzalez, M. Alcoutlabi, J.A. Ortega, The Performance of SiO_2 and TiO_2 Nanoparticles as Lubricant Additives in Sunflower Oil, Lubricants 8 (2020) 10, https://doi.org/10.3390/lubricants8010010.
[18] Y. Gao, G. Chen, Y. Oli, Z. Zhang, Q. Xue, Study on tribological properties of oleic acid-modified TiO_2 nanoparticle in water, Wear 252 (2002) 454–458, https://doi.org/10.1016/S0043-1648(01)00891-2.
[19] G. Rajakumar, A. Rahuman, S. Roopan, G. Khanna, G. Elango, D.C. Kamaraj, A. Zahir, V. Kanayairam, 3. Fungus-mediated biosynthesis and characterization of TiO_2 nanoparticles and their activity against pathogenic bacteria, Spectrochim. Acta A Mol. Biomol. Spectrosc. 91 (2012) 23–29, https://doi.org/10.1016/j.saa.2012.01.011.
[20] J.J. Healy, J.J. de Groot, J. Kestin, The theory of the transient hot-wire method for measuring thermal conductivity, Physica B+C 82 (1976) 392–408, https://doi.org/10.1016/0378-4363(76)90203-5.
[21] K.I. Nasser, J.M. Liñeira del Río, E.R. López, J. Fernández, Synergistic effects of hexagonal boron nitride nanoparticles and phosphonium ionic liquids as hybrid lubricant additives, J. Mol. Liq. 311 (2020), https://doi.org/10.1016/j.molliq.2020.113343.
[22] J.M. Liñeira del Río, E.R. López, M. González Gómez, S. Yáñez Vilar, Y. Piñeiro, J. Rivas, D.E.P. Gonçalves, J.H.O. Seabra, J. Fernández, Tribological Behavior of Nanolubricants Based on Coated Magnetic Nanoparticles and Trimethylolpropane Trioleate Base Oil, Nanomaterials 10 (2020) 683, https://doi.org/10.3390/nano10040683.
[23] J.P. Vallejo, J.M. Liñeira del Río, J. Fernández, L. Lugo, Tribological performance of silicon nitride and carbon black Ionanofluids based on 1-ethyl-3-methylimidazolium methanesulfonate, J. Mol. Liq. 319 (2020), https://doi.org/10.1016/j.molliq.2020.114335.
[24] J.M. Liñeira del Río, E.R. López, D.E.P. Gonçalves, J.H.O. Seabra, J. Fernández, Tribological properties of hexagonal boron nitride nanoparticles or graphene nanoplatelets blended with an ionic liquid as additives of an ester base oil, Lubr. Sci. 33 (2021) 269–278, https://doi.org/10.1002/ls.1543.
[25] J.M. Liñeira del Río, E.R. López, J. Fernández, F. García, Tribological properties of dispersions based on reduced graphene oxide sheets and trimethylolpropane trioleate or PAO 40 oils, J. Mol. Liq. 274 (2019) 568–576, https://doi.org/10.1016/j.molliq.2018.10.107.
[26] U. Maurya, V. Vasu, D. Kashinath, Three-way compatibility study among Nanoparticles, Ionic Liquid, and Dispersant for potential in lubricant formulation, Materials Today: Proceedings 59 (2022) 1651–1658, https://doi.org/10.1016/j.matpr.2022.03.329.

[27] V. Saini, J. Bijwe, S. Seth, S.S.V. Ramakumar, Interfacial interaction of PTFE submicron particles in oil with steel surfaces as excellent extreme-pressure additive, J. Mol. Liq. 325 (2021), https://doi.org/10.1016/j.molliq.2020.115238.
[28] J. Kałużny, A. Świetlicka, Ł. Wojciechowski, S. Boncel, G. Kinal, T. Runka, M. Nowicki, O. Stepanenko, B. Gapiński, J. Leśniewicz, P. Błaszkiewicz, K. Kempa, Machine Learning Approach for Application-Tailored Nanolubricants' design, Nanomaterials 12 (2022) 1765.
[29] B. Hamrock, D. Dowson, Minimum film thickness in elliptical contacts for different regimes of fluid-film lubrication, Proceedings of the Society of Photo-Optical Instrumentation Engineers (1978).
[30] D.E.P. Gonçalves, J.M. Liñeira del Rio, M.J.P. Comuñas, J. Fernández, J.H.O. Seabra, High Pressure Characterization of the Viscous and Volumetric Behavior of Three Transmission Oils, Ind. Eng. Chem. Res. 58 (2019) 1732–1742, https://doi.org/10.1021/acs.iecr.8b05090.
[31] D. Zhu, Q.J. Wang, On the λ ratio range of mixed lubrication, Proceedings of the Institution of Mechanical Engineers, Part J: Journal of Engineering Tribology 226 (12) (2012) 1010–1022.
[32] K. Sharif, H. Evans, R. Snidle, Modelling of elastohydrodynamic lubrication and fatigue of rough surfaces: The effect of lambda ratio, Proceedings of the Institution of Mechanical Engineers 226 (2012) 1039–1050, https://doi.org/10.1177/1350650112458220.
[33] H.A. Spikes, Mixed lubrication — an overview, Lubr. Sci. 9 (1997) 221–253, https://doi.org/10.1002/ls.3010090302.
[34] G. Guangteng, H.A. Spikes, An Experimental Study of Film Thickness in the Mixed Lubrication Regime. in: D. Dowson, C.M. Taylor, T.H.C. Childs, G. Dalmaz, Y. Berthier, L. Flamand, J.M. Georges, A.A. Lubrecht, (Eds.), Tribology Series, Elsevier, 1997, pp. 159–166, doi: 10.1016/S0167-8922(08)70445-0.
[35] R. González, A.H. Battez, J.L. Viesca, A. Higuera-Garrido, A. Fernández-González, Lubrication of DLC coatings with two tris(pentafluoroethyl) trifluorophosphate anion-based ionic liquids, Tribol. Trans. 56 (2013) 887–895, https://doi.org/10.1080/10402004.2013.810319.